International Journal of Radiology and Diagnostic Imaging

E-ISSN: 2664-4444
P-ISSN: 2664-4436
www.radiologypaper.com
IJRDI 2024; 7(2): 67-76
Received: 01-03-2024
Accepted: 06-04-2024

Eman Magdy Shaaban El Sharkawy
Department of Radiodiagnosis and Medical Imaging, Faculty of Medicine, Tanta University, Tanta, Egypt

Khaled Ismael Abd El-Gawad Elshafey
Department of Radiodiagnosis and Medical Imaging, Faculty of Medicine, Tanta University, Tanta, Egypt

Mohamed Adel ELTomy
Department of Radiodiagnosis and Medical Imaging, Faculty of Medicine, Tanta University, Tanta, Egypt

Amr Ahmed Mubarak
Department of Radiodiagnosis and Medical Imaging, Faculty of Medicine, Tanta University, Tanta, Egypt

Corresponding Author:
Eman Magdy Shaaban El Sharkawy
Department of Radiodiagnosis and Medical Imaging, Faculty of Medicine, Tanta University, Tanta, Egypt

Diffusion-weighted magnetic resonance imaging in characterization of pediatric neck masses

Eman Magdy Shaaban El Sharkawy, Khaled Ismael Abd El-Gawad Elshafey, Mohamed Adel ELTomy and Amr Ahmed Mubarak

DOI: https://doi.org/10.33545/26644436.2024.v7.i2a.388

Abstract
Background: In paediatric patients, neck masses frequently seen. Quick and accurate diagnosis directly affects treatment success. Characterizing neck masses has been done using diffusion-weighted magnetic resonance imaging. It is anticipated that the apparent diffusion coefficient (ADC) will change depending on the lesion's cellular densities.
Aim of the Work: This research aimed to evaluate the use of diffusion-weighted magnetic resonance imaging (DW-MRI) for the characterization of paediatric neck masses.
Patients and Methods: this work involved thirty pediatric participants (14 males and 16 females) with their ages ranged from 7-17 years. In 12 instances, the final diagnosis was verified by histological analysis; in the other cases, it was verified by radiographic and clinical correlation. All participants had convectional MRI, DWI-MRI with calculating value of ADC were performed.
Results: value of ADC for total 30 patients was range from 0.46 to 2.77 ($\times10^{-3}$ mm²/s), with mean 1.32 ± 0.65. Visual assessment of DW-MRI is able to distinguish between benign and cancerous lesions. There was 11 benign non inflammatory with ADC value mean ± sd (1.34±1.0) ($\times10^{-3}$ mm²/s), 18 children had benign inflammatory with ADC value mean ± sd (1.32±0.34) ($\times10^{-3}$ mm²/s) and 1 malignant case with ADC value (1.15 $\times10^{-3}$ mm²/s).
Conclusion: A novel and promising noninvasive imaging method for characterising paediatric neck masses is DW-MRI, which may assist in distinguishing between benign and malignant tumours. Therefore, DW-MRI of paediatric neck masses may be integrated into standard MR imaging.

Keywords: Apparent diffusion coefficient, DWI, neck masses, pediatric

Introduction

Because of their great anatomical and functional complexity, the head and neck regions provide significant challenges for precise regional tumour staging and diagnosis. A clinical examination may identify numerous lesions, but imaging methods are also required to accurately characterise biological aggressiveness and to improve staging and therapy [1].

A frequent cause for presenting to the paediatric emergency room is neck masses. About half of young infants have palpably normal cervical lymph nodes, complicating the clinical approach to this wide differential diagnosis, while parental worry often centres on probable malignancies [2].

Acquired and congenital neck masses are the two main groups into which paediatric neck masses may be classified, providing a strong differential diagnosis. Thyroglossal duct cysts, Branchial cleft cysts, cystic hygromas, dermoid cysts, laryngoceles, hemangiomas, teratomas, and ranulas are examples of congenital neck masses. Thyroid nodules, cancer, goitre, Epstein-Barr virus (EBV), cytomegalovirus (CMV), Bartonella, lymphoma, human immunodeficiency virus (HIV), toxoplasmosis, neuroblastoma, rhabdomyosarcoma, or melanoma are examples of acquired masses. The most frequent aetiology of cervical lymphadenopathy amongst these pathologic reasons is infection [3].

For individuals with a neck mass, prompt and precise diagnosis is critical to the outcome of their therapy. The mortality and morbidity of a disease are increased when a malignant tumour is not detected in a timely or sufficient manner [4].

Following plain-film radiography, ultrasonography is the second most popular imaging technique used in hospitals globally. Ultrasound is becoming more and more significant in head and neck imaging, with modern high-resolution ultrasound having outstanding spatial and contrast resolution for the near field [5].

Because paediatric imaging requires doctors to be wary of radiation exposure, ultrasonography (US) is often used initially. Computed tomography (CT) and MRI may be used for further acquisition if necessary. Because high frequency probes are often employed to evaluate superficial disorders, these modalities may help improve diagnostic confidence and give further insight about the involvement of deeper tissues. This is particularly important since the US penetration depth is limited to this depth [6].

In terms of tissue contrast, sensitivity of intrinsic flow, and non-ionizing radiation, MRI is superior than CT in these respects [7].

While traditional MRI primarily gives structural data, including tumour size, location, and morphological characteristics, it fails to offer information on the histology criteria, tumour grade, or tumour aggressiveness [8].

MRI assesses a lesion's shape, intensity of signal, and enhancement pattern. None of these techniques, nevertheless, can reliably distinguish between benign and malignant tumours. This has made the need to investigate novel diagnostic techniques necessary. One method that may be acquired is non-contrast enhanced technique, DW-MRI because of its sensitivity to respiratory, cardiac, and peristaltic movements, this technique's employment in the central nervous system was restricted in its early stages. However, DW echo planar MRI may now be used effectively even in other regions with significant susceptibility artefacts due to advancements in the technology of echo planar imaging as a rapid MRI sequence [9].

DWI is a MRI method that allows the apparent diffusion coefficient (ADC) value to be calculated from the diffusion characteristics of water. There is an inverse relationship between cellularity changes and ADC alterations. Particularly in highly cellular tissues, cell membranes restrict the diffusion of extracellular water, resulting in low ADC values. When diffusion is enhanced in tissues with poor cellularity (Such as necrotic or edematous tissue), ADC measurements are high [10].

In addition to being a popular research topic, DWI is currently commonly employed in a number of clinical situations. In addition to being a popular research topic, DWI is currently commonly employed in a number of clinical situations. It has been evaluated in almost all malignancies, such as cancer of the head and neck, for recognizing recurrent or residual tumours during follow-up assessments, for distinguishing malignant from benign lesions, and to differentiate distinct malignant histotypes or tumour grades [11].

Adult neck masses have recently been characterized using DW MRI. While some researches discovered a negative correlation between the cellularity of the masses and the ADC value, other researchers concluded that the ADC value was not a valid way to distinguish benign from malignant tumours in paediatric patients [12].

Aim of the study
To assess the role of DW-MRI in characterization of pediatric neck masses.

Patients and Methods
This prospective work had been on performed 30 pediatric patient (14 males and 16 females), ranging in age from 7-17 years, patients were subjected to MRI for diagnosis of neck mass at Tanta University Radiology Department during a period of 2 years that started from June 2021 till June 2023.

Inclusion criteria
All pediatric patients either males or females presented with neck masses, who were diagnosed either clinically or by Ultrasonography.

Exclusion criteria
- Individuals who have had prior biopsies, surgery, or medical intervention via radiotherapy or chemotherapy.
- Individuals who have contraindication to perform MRI including.

a) Individuals with intraocular metallic foreign body.
b) Individuals with cardiac pacemakers.
c) Individuals with intracranial aneurysm clips.
d) Individuals known to have claustrophobia.

Ethical consideration
- An informed consent was signed from each patient's caregiver to be included in the current work.
- Patients and their families were well-informed about the procedure, with all potential advantages and possible complications and side effects.
- All data were confidential.

Patients included in this study were subjected to the following
Comprehesive taking of history includes
- Age.
- Sex.
- Underlying disease.
- Onset, course and duration of the swelling.
- History of previous intervention.
- Past history of related illness.
- Family history of any malignancies.

Clinical examination: including general and systemic examination

Ultrasonographic examination for all patients was done on abdomen, pelvis and neck which was done using superficial probe.

MRI examination.

Equipment
- Patients were examined using closed MRI Systems (1.5 Tesla) Signa Explorer GE healthcare, USA.
- Throughout the examination, patients were in supine position utilizing standard head and neck coil,
- To obtain the highest quality MRI, 11 patients were given anesthesia and 19 child received sedation via an IV line by a specialized anesthetist.

MRI examination protocol
Each participant underwent the predefined examination programme, which involved the following.

A. Conventional MRI
Axial T_1 spin echo with no fat suppression, Axial T_2 turbo spin echo (TSE) with no fat suppression, Coronal T_2 sequence with fat suppression, and Axial T_1 sequence with fat suppression were among the sequences used in the MRI scan. For T_1 and T_2-weighted pictures, the corresponding

values for repetition time (TR), echo time (TE), and number of excitations were (600/20/2) and (4000/90/4). 18 cm is the field of view (FOV), 256 x 256 matrix, 2 mm for slice thickness, and 1 mm for the interslice gap.

B. DW-MRI examinations

Single shot spin echo planar imaging (SS-EPI) in the axial plane was used to create the DWI, and chemical shift specific fat suppression was used to suppress fat.

The "short" echo time (TE) of 100 ms, the "High" repetition time (TR) of 1700 ms, the "Coarse" matrix of 192 x 144, the FOV of 25 cm, the slice numbers of 30, the slice thickness of 5 mm, the inter-slice gap of 2.5 mm, and the acquisition duration of around 1 minute and 45 seconds were used to achieve diffusion. In the axial plane, three b-factors, namely 0, 500, and 1000 s/mm2, were determined. An ADC map was acquired.

C. Contrast enhanced MRI

When 0.2 ml/kg of body weight of gadopentate and dimeglumine were injected intravenously, axial and coronal planes of MRI weighted images (TR/TE of 800/15 ms) were gained.

DW MRI analysis

Qualitative analysis

It alludes to an evaluation of the masses' intensity of signal visually. Every lesion was assessed based on its location, size, extent, and relationship to nearby structures. Based on the signal intensity of nearby skeletal muscles, the masses were categorized as having a low DWI signal or a high DWI signal. Correlations were found between the mass signal on DWI and the matching signal on the automatically produced ADC maps. While limited diffusion was observed as high signal on high b value (1000) DWI and low signal on matching ADC map, masses with free diffusion displayed low signal on DWI and high signal on ADC map. High signal was shown by masses with T_2 shine via effects in both DWIs and ADC maps.

Quantitative analysis

Finding a circular ROI 1-2 cm within the mass (avoid cystic areas with mixed lesions by correlation with T_2WI and post contrast T_1WI) and obtaining three ADC values were used to do the quantitative evaluation. The mean ADC value was then computed.

5- The final diagnosis was confirmed by histopathological examination in 12 cases, 6 of them by aspiration, other 6 surgical excision and for the other cases, through clinical and radiological correlation.

Statistical analysis and data interpretation

SPSS (Statistical Package for the Social Science; SPSS Inc., Chicago, IL, USA) version 23 was used to input and analyse the data. Numbers and percentages were used to describe the qualitative data. After utilising the Shapiro-Wilk test to confirm normality, quantitative data was obtained utilizing the median (Minimum and maximum) for nonparametric data and the mean and standard deviation for parametric data.

Receiver operating characteristic (ROC) curve analysis was used to assess a test's accuracy or diagnostic performance. From the curve, both specificity and sensitivity were identified, and cross-tabulation was used to determine PPV, NPV, and accuracy. Utilising the one-way ANOVA (analysis of variance) test and the two-tailed Student's t test, or for quantitative data as appropriate, the significance of the variation among the groups was established. Qualitative parameters were evaluated utilising chi-squared χ^2test.

The acquired findings were deemed significant at the 0.05 level. "Probability (P-value)"

- P-value more than 0.05 was deemed insignificant.
- *P-value <0.05 was deemed significant.
- **P-value <0.001 was deemed as highly significant. The diagnostic sensitivity, specificity was calculated as follows (Table 1).

Table 1: Significance of "Probability (P-value)"

Reference test	Evaluated test		Total
	+ ve	- ve	
+ ve	True + ve (a)	False -ve (c)	A + c
- ve	False + ve (b)	True -ve (d)	B + d
Total	A + b	C + d	A + b + c +d

Where

Sensitivity: described as the ability of a certain method or finding out that the largest percentage of people were really ill.

Sensitivity = a / (a +c) ×100.

Specificity: is the ability of a test to be consistently negative in the absence of the illness and to avoid providing false-positive findings.

Specificity = d / (b + d) ×100.

Positive predictive value = a / (a +b) ´100.

Negative predictive value = d / (c +d) ´100.

Results

This study had been carried out on 30 pediatric patients presented with neck mass. Patients were assembled from Radiodiagnosis Department at Tanta University. Fourteen of them (46.7%) were males and 16 (53.3%) patients were females, their mean age was 12.87±3.51 years, ranging from 7 - 17 years.

As regard to associated symptoms plus neck swelling for total 30 patients, the most common presentation was dysphagia 17 cases 56.7%. According to site of the lesion, the most common site seen was Submandibular space 6 cases 20%, followed by mouth floor, peri auricular and carotid space were 5 cases 16.7%, the lowest presentation was parapharyngeal space 1 case 3.3%.

According to MRI signal intensity for total 30 patients. Hypo-intense signal was elected in 25 cases 83.3% at T_1WI. While Isointense signal was presented at T_2WI in 6 cases 20%. Hyper-intense signal was seen at T_1WI and T_2WI in (5 case 16.7%, & 24 cases 80%) of lesions respectively as shown in (Figure 1). The commonest enhancement pattern of the lesions in post contrast MRI images was the peripheral enhancement in 22 cases 73.3%, followed by homogenous enhancement in 8 cases 26.7% of cases. The masses were cystic in 25 cases and solid in 5 cases (83.3%, 16.7%) respectively, and the superficial and deep mass were 21 and 9 cases (70%, and 30%) respectively with well-defined margin and ill-defined margin were 26 and 4 cases (86.7%, and 13.3%) respectively

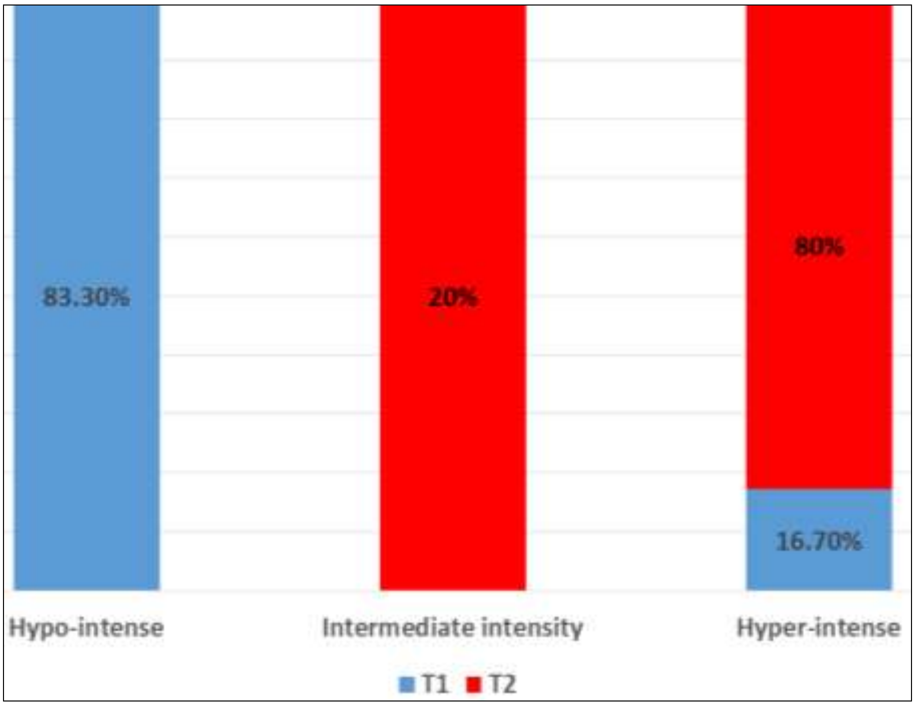

Fig 1: Distribution of the cases of the study based on to T_1 and T_2 (n = 30)

According to diffusion weighted MRI imaging of the mass for total 30 patients, restricted diffusion was encountered in 25 cases where as free diffusion was encountered in remaining 5 cases, (83.3%, and 16.7%) respectively as shown in (Table 2).

Table 2: Distribution of the cases of the study based on diffusion weighted MRI of the lesion (n = 30)

	No.	%
Diffusion		
Restricted	25	83.3
Free	5	16.7

Quantitative analysis of ADC maps for 30 patient revealed that ADC value of the lesions ranged from 0.46 to 2.77 ($\times 10^{-3}$ mm²/s), with a mean of 1.32 ± 0.65 as displayed in (Table 3).

Table 3: Descriptive analysis of the cases of the study based on ADC value of the lesions (n = 30)

	Min. - Max.	Mean ± SD.	Median (IQR)
ADC value ($\times 10^{-3}$ mm²/s)	0.46-2.77	1.32±0.65	1.12 (1.05-1.48)

IQR: Inter quartile range SD: Standard deviation

Regarding to the relation between ADC value and diffusion weighted MRI, it was significantly higher in free diffusion, the mean was 2.50 ± 0.37 compared to patients with restricted diffusion where the mean was 1.08 ± 0.36, with P value <0.001 as shown in (Table 4).

Table 4: Relation between ADC value with Diffusion (n = 30)

	No.	ADC value ($\times 10^{-3}$ mm²/s)		U	p
		Mean ± SD.	Median (Min. - Max.)		
Diffusion					
Free	5	2.50±0.37	2.77 (2.09 - 2.77)	0.000*	<0.001*
Restricted	25	1.08±0.36	1.09 (0.46 - 1.48)		

SD: Standard deviation U: Mann Whitney test

p: p value for Relation between ADC value with Diffusion

*: Statistically significant at p ≤ 0.05

According to histopathology Benign inflammatory lesions were 18 cases 60%, benign non-inflammatory lesions 11 cases 36.7%, malignant lesions 1 case 3.3% as shown in (Table 5).

Table 5: Distribution of the cases of the study based on nature of the lesion (n = 30)

Nature of the lesion	No.	%
Benign inflammatory	18	60.0
Benign non-inflammatory	11	36.7
Malignant	1	3.3

Regarding to the relation between ADC value and nature of the lesion, high ADC value was seen in benign lesions, lowest ADC value was seen in malignant lesions, as shown in (Figure 2).

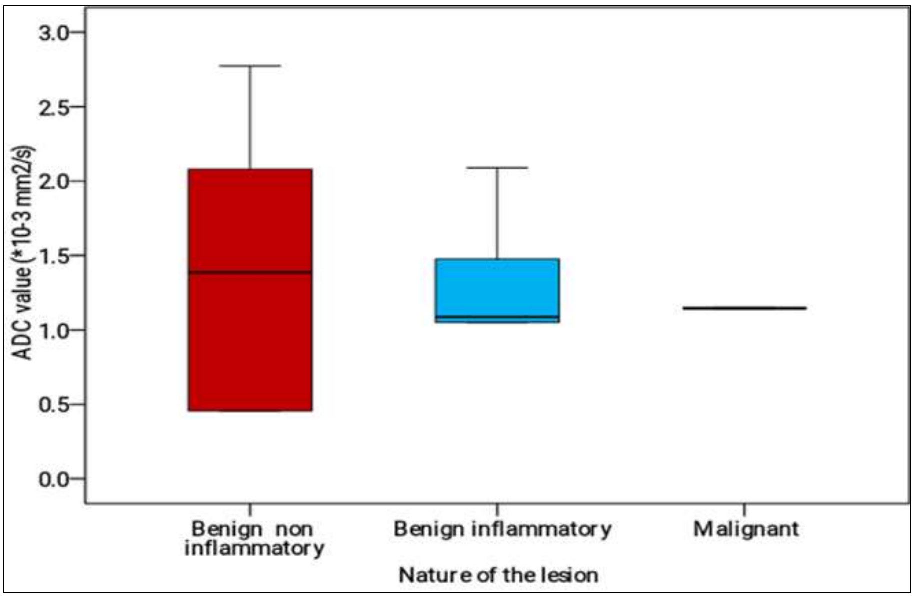

Fig 2: Box plot graph of the studied cases according to ADC value and nature of the lesion (n = 30)

Case presentation

Case 1: A 7 years old male patient presented with painful swelling in the left periauricular region, MRI findings showed in (Figure 3).

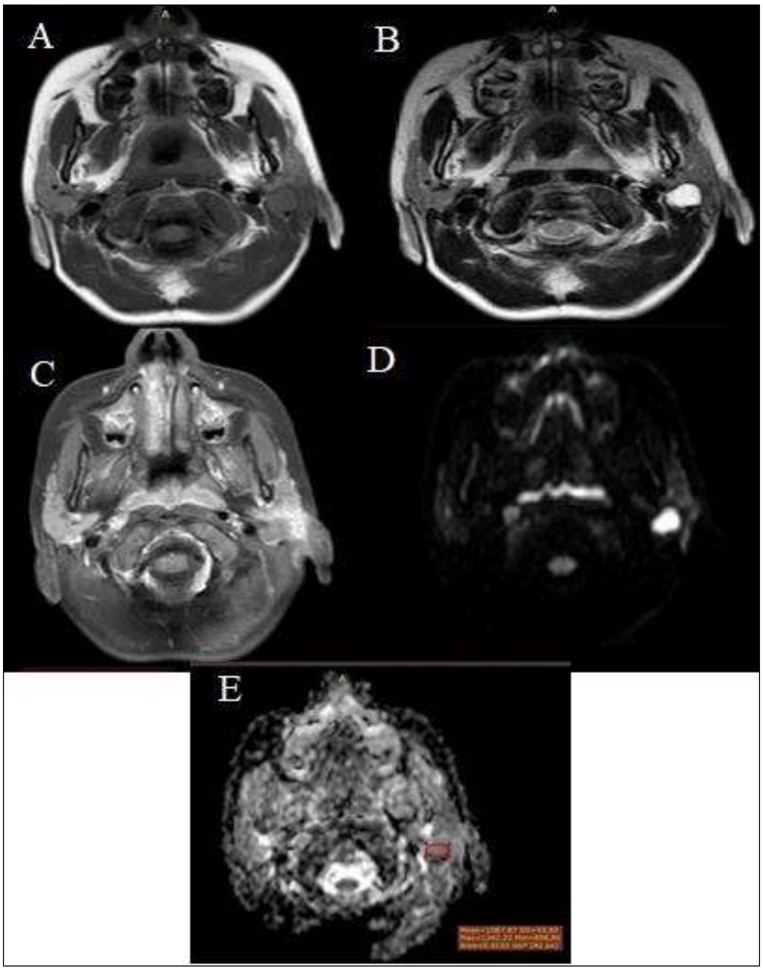

Fig 3: MRI findings were: (A) a well-defined cystic lesion related to Superficial lobe of left parotid gland appear low signal intensity at T_1WI, (B) high signal intensity at T_2WI, (C) peripheral enhancement at fat suppressed T_1 with contrast, (D) seen restricted on DWI, (E) with ADC value estimated to be 1.087×10^{-3} mm² /s.

MR diagnosis: infected 1st branchial cleft cyst

Case 3

15 years old female patient presented with painful left neck swelling. MRI findings showed in (Figure 4).

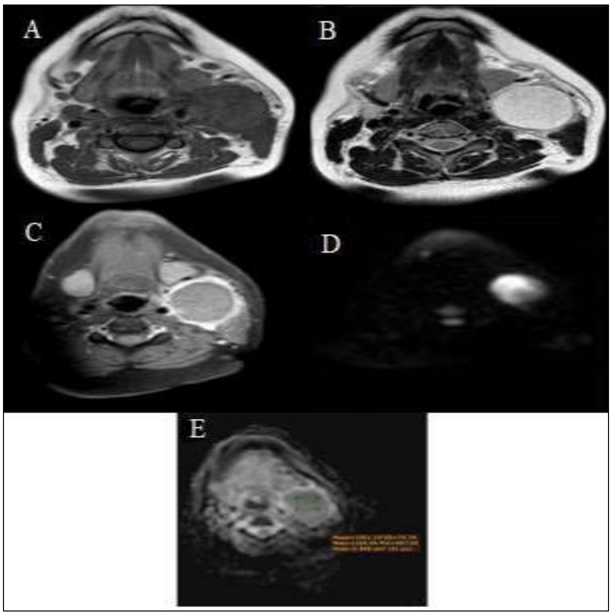

Fig 4: MRI findings: (A) a Well-defined cystic lesion at left carotid Space appear low signal intensity at T_1WI, (B) high signal intensity at T_2WI, (C) thick marginal enhancement at post contrast fat suppressed T_1WI, (D) seen restricted on DWI, (E) with ADC value estimated to be 1.051×10^{-3} mm²/s (E)

MR diagnosis: Infected second branchial cleft cyst.

Case 4

13 years old male patient with history of mucoepidermoid carcinoma underwent surgical excision, presented with dysphagia. MRI findings showed in (Figure 5).

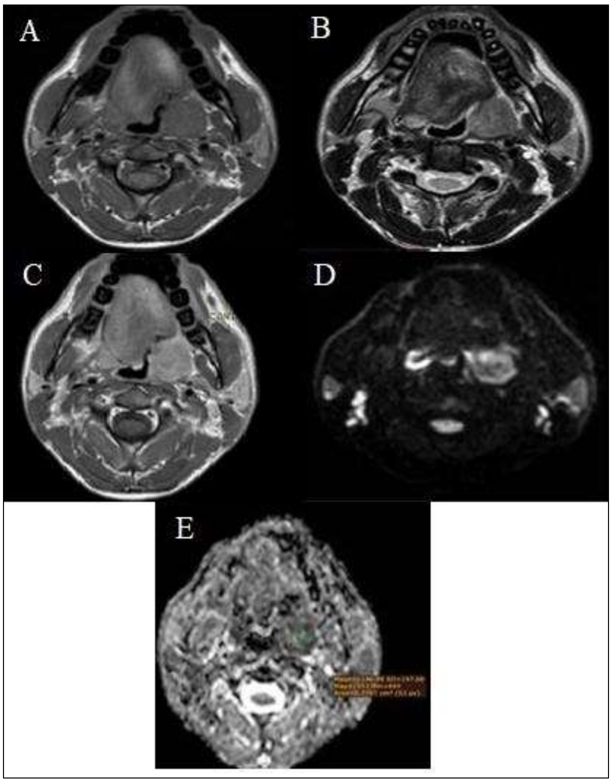

Fig 5: MRI findings: (A) Mass at left Para pharyngeal space that appears low signal intensity at T_1WI, (B) intermediate signal intensity at T_2WI, (C) with homogeneous enhancement at T_1WI with contrast, (D) seen restricted on DWI, (E) with ADC value estimated to be 1.146×10^{-3} mm²/s MR diagnosis: recurrent mucoepidermoid carcinoma

Case 5

12 years old female patient with fever and painful swelling at the left side of the neck. MRI findings showed in (Figure 6).

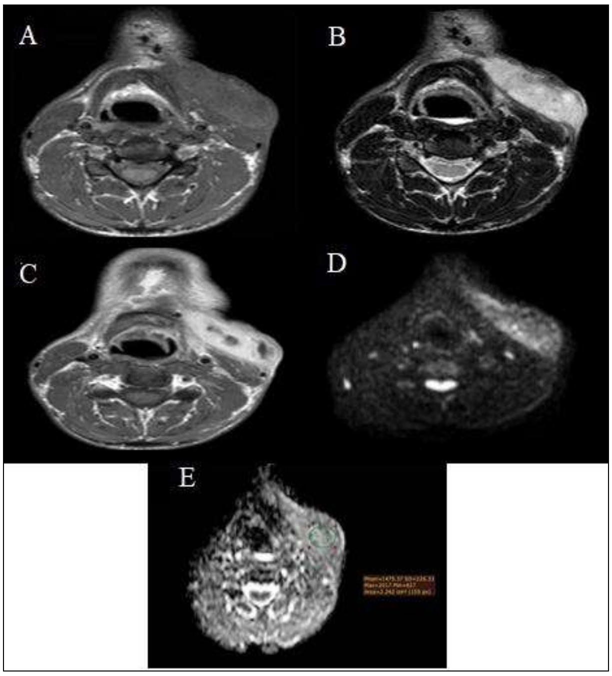

Fig 6: MRI findings: (A) Thick walled fluid collection at the left side of the neck that appears low signal intensity at T_1WI, (B) high signal intensity at T_2WI, (C) with thick marginal enhancement at T_1WI, (D) seen restricted on DWI, (E) with ADC value estimated to be 1.475×10^{-3} mm² /s

MR diagnosis: Subcutaneous abscess at the left submandibular space.

Case 6

16 years old female patient with mouth floor swelling. MRI findings showed in (Figure 7).

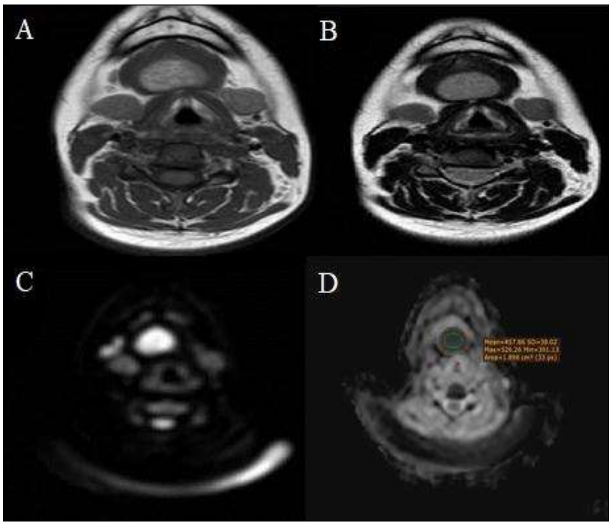

Fig 7: MRI findings: (A) a well-defined mouth floor cystic lesion that elicit high signal intensity at T_1WI, (B) intermediate signal intensity at T_2WI, (C) seen with restricted diffusion on DWI, (D) with low signal at ADC map with ADC value estimated to be 0.457×10^{-3} mm² /s

MR diagnosis: Sublingual epidermoid cyst.

Discussion

Neck masses, a common occurrence in pediatrics, can be caused by various conditions, ranging from congenital to vascular, and their prevalence varies from common to rare [13].

The clinical diagnosis of cervical lymphoma in young children is complicated by the presence of palpable normal nodes, and parental anxiety often focuses on potential malignancy [2].

Rapid development of diagnostic imaging technology offers new facilities for evaluating neck masses in children, with conventional methods like ultrasonography and CT being increasingly important due to cost and ease of use [4].

Conventional MRI techniques use T_1W, T_2W, FST_2W, and CE-T_1W sequences for identifying anatomical features and characterising lesions [13].

T_1W imaging best reveals perilesional anatomy, T_2W for tumor conspicuity, multi-planar reconstructions for nerve long axis, CE-T_1W for tumor vascularity, cystic or hemorrhagic changes [14].

DW-MRI, first used in 2001, has shown promise in identifying various types of lesions, including lymphomas, carcinomas, benign cysts, benign salivary gland tumors, and metastatic lymphadenopathy [15].

This work aimed to assess the role of DW-MRI in characterization of pediatric neck masses.

This work was conducted over 2 years with 30 pediatric patients who experienced a neck mass. The participants were recruited from the Radiology Department at Tanta University.

DWI and ADC maps were created for each individual using two distinct b-values (0 and 1000 s/mm2) and diffusion-sensitive gradients applied across three orthogonal directions (x, y, and z).

The mean age of enrolled patients was 12.87±3.51 years, with ranging from 7 - 17 years. There were 14 (46.7%) male and 16 (53.3%) female. In contrast to our findings, Friedman *et al*., (2019) [2] study aimed to assess the time and agreement between paediatric emergency doctors' point-of-care ultrasound (POCUS) and radiology department images for children with neck masses. The mean age of the 75 participants was 7±7 years, with 39 (52%) male and 36 (48%) female patients.

The research conducted by Agarwal *et al*., (2001) [16] examined neck mass in 86 youngsters, of whom 34 (40%) were males and 52 (60%) were females. The male to female ratio was 1:1.5, with a preponderance of females.

Parents are more concerned about neck masses than youngsters who have them because the majority don't show any symptoms. On the other hand, infected lymph nodes or cysts hurt and are painful, and they might raise fever. There are also many other symptoms that may be present Balakrishnan *et al*., (2012) [17].

In the present study, regarding associated symptoms with a neck swelling for a total of 30 patients, the most common presentation was dysphagia at 56.7%, followed by general toxic symptoms at 53.3%, dyspnea at 16.7%, cough at 10%, and hoarseness of voice at 6.7%.

In Côrte *et al*., (2017) [18] study, the two most common signs/symptoms were odynophagia (50.6%) and fever (63.9%). In the study conducted by Meyer *et al*., (2009) [19], the symptoms that were most frequently mentioned were odynophagia or sore throat (35.0%), pain in the neck (48.0%), stiffness in the neck (42.9%), neck or face swelling (28.2%), and reduced oral intake (24.3%).

Based on the site of the lesion, the present study revealed that lesions were confined to Submandibular space were 20%, Mouth floor, Periauricular and carotid space were16.7%, paraglottic space and Posterior cervical space were 10%, Larynx was 6.7%, parapharyngeal space 3.3%.

In comparison to the study done by Abdel Razek *et al*. (2009) [13], which included a total of 78 pediatric patients, the masses were found in various locations including the visceral space (14.4%), parotid space (12.4%), submandibular region (10.9%), sublingual space (7.8%), paranasal sinus (5.4%), nasal cavity (4.6%), parapharyngeal space (3.9%), retropharyngeal space (3.9%), posterior cervical space (3.1%), and masticator space (3.1%).

On traditional T_1-weighted scans, lesions containing bone, air, thick calcification, or fast blood flow may show up as absolute signal voids. Sarcomas and other aneurysms, calcified lesions, odontogenic or bone-forming masses, paragangliomas (Although mixed with solid tissue), and arteriovenous malformations of the head and neck can all cause signal voids. On T_1-weighted MRI, very hyperproteinaceous secretions (concretions) or rhinoliths might occasionally show a signal void [20].

Due to the edoema that goes along with most inflammatory lesions of the head and neck, these lesions appear hyperintense on T_2-weighted scans. These vivid inflammatory signs include mucosal thickness, abscesses, and fluid levels from acute sinusitis. On T_2-weighted scans, the majority of cysts (Mucous retention cysts, ranulas, thyroid cysts, branchial cleft cysts, and so forth) and numerous benign masses (Polyps, pleomorphic adenomas, lymph nodes, hemangiomas, and so forth) are bright [20].

Based on the tissue's composition, pathological lesions can have a wide variety of signal intensities. Malignant and benign solid tumours will have intensities in between those of muscle and fat, and they will get more intense as the pulse sequence's T_2-weighting increases. Granulation tissue and inflammatory tissue can seem identical, making it impossible to differentiate cancer from infection or acute/subacute surgical changes based just on tissue signal intensities. On all pulse sequences, the signal strength of chronic fibrosis will be modest [21].

In our study, the signal intensity for total 30 patients. Hypo-intense was presented by 83.3% in T_1 and no cases in T_2. While no isointensity cases in T_1 and 20% in T_2. Hyper-intense was (16.7% and 80%) in T_1 and T_2 respectively.

In Agarwal *et al*., (2011) [16] study, Low to moderate signal aberrations in the subcutaneous tissues were detected by MRI images; these abnormalities failed to improve when gadolinium was administered. And in Das *et al*., (2016) [21] study, all masses were hypo- to isointense to adjacent muscle on T_1 images and heterogeneously hyperintense on T_2.

According to enhancement pattern of the lesions in post contrast MRI images, our study showed that the commonest pattern was the Peripheral enhancement in 73.3%, followed by homogenous enhancement in 26.6% of cases.

Yoon *et al*., (2013) [22] study, in 54% (11/24) of the participants with neck abscesses, rim augmentation more than 50% of the circumference was seen, according to the study.

Information that is helpful is provided by the mass's consistency. Multiple tiny lymph nodes are referred to as lymphadenopathy. This often indicates reactive lymphadenopathy in the neck caused by an upper respiratory tract infection. A firm, rubbery mass that is immovable or adhered to the deep tissues of the neck, or a hard, irregular mass, might be signs of cancer [23].

Regarding to consistency, our study found that masses were cystic and solid in 83.3% and 16.7% patients respectively. Abdel Razek *et al*., (2009) [13] study was in the same line with our results, their studied masses were cystic and solid in 77.7% and 22.3% patients respectively.

In children, neck mass involving both superficial and deep neck spaces are common. In children, superficial palpable masses of the neck and head are prevalent; most of these lesions turn out to be benign in the end [12].

In our study, as regard to the depth of mass, superficial and deep masses were (70%, and 30%) respectively. This result was in disagreement with the work performed by Wetmore *et al*., (1998) [24], which was conducted on 66 participants, 33 with superficial and 33 with deep neck masses.

According to the margin of the mass, our study had classified the masses as well-defined and ill-defined from total 30 patients, well defined margin and ill-defined margin were (86.7%, and 13.3%) respectively.

Similarly, to our results, the study done by Gupta, (2023) [25], who had 87% of neck masses was with well-defined margin and ill-defined margin was presented by 13% of masses.

Also in Kim *et al*., (2005) [26] study, it was a study to evaluate the CT and MRI outcomes of masses in the neck. Most of masses were with well-defined margin. While Das *et al*., (2016) [21] study, showed that all tumors had well-defined margins with round or fusiform configuration.

DWI provides useful information that enhances lesion characterisation. However, in addition to tissue cellularity, the lesion's histological background can have a big impact on its diffusion properties. As a result, limited diffusion may be seen in benign tumours with unusual histology, potentially resulting in diagnostic mistakes Das *et al*., (2016) [21].

In our study, the DWT analysis revealed that 83.3% of the masses exhibited restricted diffusion, while 16.7% showed free diffusion. This finding contradicts the findings of Das *et al*. (2016) [21] work, that stated different percentages. Specifically, out of the forty-two masses were analyzed, only one showed uniformly restricted diffusion, while the remaining showed free diffusion.

Determining the ADC value from DWI can be useful in the diagnosis of subcentimeter nodal metastases and in the staging of cancer. Additionally, the ADC value separates benign lesions from malignant tumours, tumour necrosis from abscesses, and carcinomas from lymphomas [27].

In our study, ADC value for total 30 children was ranged from 0.46 to 2.77 ($\times 10^{-3}$ mm²/s), with a mean of 1.32±0.65. Similarly, to Abou khadrah *et al*., (2019) [1] study, which evaluated solid neck and head masses using DW-MRI and discovered that the ADC values varied from 0.674 to 2.590 (×10-3 mm²/s). Also, the mean ADC values in Kanmaz *et al*., (2018) [4] study was similar to our result (1.57 $\times 10^{-3}$ mm²/s).

Only a tiny percentage of paediatrics' neck masses are malignant tumors; the majority of neck masses are benign Kanmaz *et al*., (2018) [4]. In our study, only one child had malignant lesion which was recurrent mucoepidermoid carcinoma, and the remaining children had benign lesions, 6 (20%) patients had subcutaneous abscess, 5 (16.7%) patients had infected 1st branchial cleft cyst, 5 (16.7%) patients had complicated 2nd branchial cleft cyst, and 5 (16.7%) patients had epidermoid cyst. 3 (10%) laryngocele (Mixed type), 3 (10%) lymphatic malformation and 2 (7%) laryngeal inflammation.

In contrast with our results, the work done by Kanmaz *et al*., (2018) [4]. Showed benign masses in 17 (53.1%) instances and malignant masses in 15 (46.9%) instances. The benign masses included one (3.1%) glomus tumour, one (3.1%) thyroglossal duct cyst, two (6.2%) branchial cleft cysts, 2 (6.2%) cervical sympathetic chain schwannomas, one (3.1%) tbc lymphadenitis, 3 (9.3%) reactive lymphadenopathies, 5 (15.6%) pleomorphic adenomas originated from major salivary glands, and two (6.2%) Whartin's tumours.

The aim of this work was to evaluate the usefulness of DW-MRI in differentiating between malignant and benign neck and head masses by comparing the ADC values of the two studies Kanmaz *et al*. (2018) [4]. It found a total of 17 (53.1%) benign tumours and 15 (46.9%) malignant masses.

While in Abdel Razek *et al*., (2009) [13] study, A prospective research including 78 consecutive paediatric patients was conducted. In 28 cases, the ultimate diagnosis was malignant tumours, whereas 48 individuals had benign masses.

Studies on the application of DW-MRI for inflammatory disorders and benign neck pathologies are quite rare in the literature. The cellularity and matrix of tumours, as well as some overlap between certain malignant and benign lesions, are some of the complicated aspects that affect the ADC itself Razek *et al*., (2008) [28].

The distinction between benign and malignant lesions, as seen by variations in diffusion time, may indicate variations in cell permeability or tissue structure. This demonstrates the possible significance of providing diffusion time for neck diffusion MRI interpretation Kanmaz *et al*., (2018) [4].

Based on histopathology, the current study found that 60% of lesions were benign and inflammatory, 36.7% were benign and non-inflammatory, and 3.3% were malignant.

When compared to Abdel Razek *et al*. (2009) [13] study, this study found that 47.4% of lesions were malignant by histopathology, 6.7% were benign and inflammatory, and 45.7%were benign and non-inflammatory. Also, Kanmaz *et al*. (2018) [4] reported that 46.9% of lesions were malignant and 53.1% were benign.

Our work recealed that the ADC value was found to be correlated with the nature of the lesion, with benign lesions exhibiting high ADC values with a mean of (1.34±1.0) ($\times 10^{3}$ mm²/s) and malignant lesions showing the lowest ADC values at (1.15 $\times 10^{-3}$ mm²/s).

Our study aligned with the findings of Abdel Razek *et al*. (2009) [13], which focused on characterizing pediatric neck and head masses utilising DW-MRI. The study revealed that the mean ADC values for malignant tumours and benign solid masses were (0.93±0.18) $\times 10^{-3}$mm²/s and (1.57±0.26) $\times 10^{-3}$ mm²/s, respectively.

Another study agreed with our result, by Baiomy *et al*. (2020) [12] focused on using DW-MRI to characterize paediatric neck and head masses. The study found that the mean ADC values for malignant tumours and benign solid masses had been (0.83±0.23) ×10-3mm²/s and (1.6)×10-3 mm²/s, correspondingly.

Also, Kanmaz *et al*., (2018) [4] study showed that the mean ADC values for malignant tumors and benign solid masses were (0.90 ±0.17)×10- 3mm²/s and (1.57±0.42)×10-3 mm²/s, correspondingly.

Conclusion

A novel and promising noninvasive imaging method for characterizing paediatric neck masses is called DW-MRI, which may be used to distinguish between benign and malignant tumours. Therefore, normal MRI of a paediatric neck mass could be enhanced using DW-MRI.

When combined with standard conventional MRI, qualitative (DW-MRI) and quantitative (ADC) assessment proved beneficial in addressing several diagnostic issues related to neck mass imaging. DWI helps to direct biopsy targets and lower the number of avoidable invasive operations.

Acknowledgement

Not available.

Author's Contribution

Not available.

Conflict of Interest

Not available.

Financial Support

Not available.

References

1. Abou Khadrah RS, Imam HH. Multiple b values of diffusion- weighted magnetic resonance imaging in evaluation of solid head and neck masses. Egypt J Radiol. Nucl. Med. 2019;50:1-10.
2. Friedman N, Tseng F, Savic R, *et al*. Reliability of Neck Mass Point-of- Care Ultrasound by Pediatric Emergency Physicians. J Ultrasound Med. 2019;38(11):2893-900.
3. Burns J, Pathania S, Griesser R, *et al*. Evaluation of a unilateral neck mass in a 16-year-old female: Kikuchi-Fujimoto disease with superimposed bacterial lymphadenitis. SAGE Open Med Case Rep. 2020;8:1-4.
4. Kanmaz L, Karavas E. The role of diffusion-weighted magnetic resonance imaging in the differentiation of head and neck masses. J Clin. Med. 2018;7(6):130.
5. Farid A, Shalaan A, Khedr S. Impact of ultrasound in diagnosis of pediatric superficial masses in head and neck. Benha Med. J. 2020;1;37:63-76.
6. Brown RE, Harave S. Diagnostic imaging of benign and malignant neck masses in children - A pictorial review. Quant Imaging Med Surg. 2016;6(5):591-604.
7. Soliman AF, Aggag MF, Abdelgawwad AE, *et al*. Role of Diffusion Weighted MRI in Evaluation of Orbital Lesions. Al-Azhar Int. Med. J. 2020;1(1):331-336.
8. Mustafa WF, Abbas M, Elsorougy L. Role of diffusion-weighted imaging in differentiation between posterior fossa brain tumors. Egypt J Neurol. Psychiatry Neurosurg. 2020;56:1-8.
9. TM, Ahmed YA, Ahmed GA. The usefulness of diffusion- weighted MRI in the differentiation between focal uterine endometrial soft tissue lesions. Egypt J Radiol. Nucl. Med. 2019;50(1):1-8.
10. Kolff-Gart AS, Pouwels PJ, Noij DP, *et al*. Diffusion-weighted imaging of the head and neck in healthy subjects: reproducibility of ADC values in different MRI systems and repeat sessions. AJNR Am J Neuroradiol. 2015;36(2):384-390.
11. Messina C, Bignone R, Bruno A, *et al*. Diffusion-weighted imaging in oncology: An update. Cancers. 2020;12(6):1493.
12. Baiomy A, Nada A, Gabr A, *et al*. Characterization of pediatric head and neck masses with quantitative analysis of diffusion-weighted imaging and measurement of apparent diffusion coefficients. Indian J Radiol Imaging. 2020;30(4):473.
13. Abdel Razek A, Gaballa G, Elhawarey G, *et al*. Characterization of pediatric head and neck masses with diffusion-weighted MR imaging. Eur. Radiol. 2009;19:201-208.
14. Mazal AT, Ashikyan O, Cheng J, *et al*. Diffusion-weighted imaging and diffusion tensor imaging as adjuncts to conventional MRI for the diagnosis and management of peripheral nerve sheath tumors: Current perspectives and future directions. Eur. Radiol. 2019;29:4123-4132.
15. Wang J, Takashima S, Takayama F, *et al*. Head and neck lesions: characterization with diffusion-weighted echo-planar MR imaging. Radiology. 2001;220(3):621-630.
16. Agarwal R, Handler S, Matthews M, *et al*. Pilomatrixoma of the head and neck in children. Otolaryngol Head Neck Surg. 2001;125(5):510-515.
17. Balakrishnan K, Edwards TC, Perkins JA. Functional and symptom impacts of pediatric head and neck lymphatic malformations: Developing a patient-derived instrument. Otolaryngol. Head Neck Surg. 2012;147(5):925-931.
18. Côrte F, Firmino-Machado J, Moura C, *et al*. Acute pediatric neck infections: Outcomes in a seven-year series. Int. J Pediatr. Otorhinolaryngol. 2017;99:128-134.
19. Meyer A, Kimbrough T, Finkelstein M, *et al*. Symptom duration and CT findings in pediatric deep neck infection. Otolaryngol. Head Neck Surg. 2009;140(2):183-186.
20. Charan I, Kapoor A, Kumar N, *et al*. Evaluation of neck mass with computed tomography: An observational study. Int. J Sci. Stud, 2014, 2(7).
21. Das A, Bhalla A, Sharma R, *et al*. Benign neck masses showing restricted diffusion: Is there a histological basis for discordant behavior? World J Radiol. 2016;8(2):174.
22. Yoon S, Yoon D, Kim S, *et al*. CT differentiation of abscess and non-infected fluid in the postoperative neck. Acta Radiol. 2013;54(1):48-53.
23. Meier JD, Grimmer JF. Evaluation and management of neck masses in children. Am Fam. Physician. 2014;89(5):353-358.
24. Wetmore R, Mahboubi S, Soyupak S. Computed tomography in the evaluation of pediatric neck infections. Otolaryngol. Head Neck Surg. 1998;119(6):624-627.
25. Gupta D. Role of high resolution ultrasonography and doppler in the evaluation of neck masses. Int. J Life Sci. Biotechnol. Pharma Res.; c2023. p. 12.
26. Kim S, Kim H, Park S, *et al*. Nodular fasciitis in the head and neck: CT and MR imaging findings. AJNR Am J Neuroradiol. 2005;26(10):2617-2623.
27. Chawla S, Kim S, Wang S, *et al*. Diffusion-weighted

imaging in head and neck cancers. Future Oncol. 2009;5(7):959-975.
28. Razek A, Megahed A, Denewer A, *et al*. Role of diffusion-weighted magnetic resonance imaging in differentiation between the viable and necrotic parts of head and neck tumors. Acta Radiol. 2008;49(3):364-370.

How to Cite This Article
El Sharkawy EMS, El-Gawad Elshafey KIA, ELTomy MA, Mubarak AA. Diffusion-weighted magnetic resonance imaging in characterization of pediatric neck masses. International Journal of Radiology and Diagnostic Imaging. 2024;7(2):67-76.